



ORIGINAL ARTICLE

Enhanced three-dimensional electrochemical process using magnetic recoverable of $\text{Fe}_3\text{O}_4@\text{GAC}$ towards furfural degradation and mineralization



Peyman Pourali^a, Mehdi Fazlzadeh^{a,b}, Morteza Aaligadri^a, Abdollah Dargahi^c, Yousef Poureshgh^{a,*}, Babak Kakavandi^{d,e,*}

^a Department of Environmental Health Engineering, School of Public Health, Ardabil University of Medical Sciences, Ardabil, Iran

^b Department of Environmental Health Engineering, School of Public Health, Tehran University of Medical Sciences, Tehran, Iran

^c Social Determinants of Health Research Center, Ardabil University of Medical Sciences, Ardabil, Iran

^d Research Center for Health, Safety and Environment, Alborz University of Medical Sciences, Karaj, Iran

^e Department of Environmental Health Engineering, Alborz University of Medical Sciences, Karaj, Iran

Received 26 February 2022; accepted 17 May 2022

Available online 21 May 2022

KEYWORDS

Electrochemical Oxidation;
Furfural;
3D electrochemical;
Particle Electron;
Granular activated carbon

Abstract Furfural is as one of the major environmental pollutants in different industrial effluents such as refinery and petrochemical, paper, cardboard and oil refining. This toxic chemical is irritant and causes allergy for skin, eyes and mucous membranes. This study was developed to investigate the efficiency of a three-dimensional electrochemical process in the presence of granular activated carbon magnetized with Fe_3O_4 ($\text{Fe}_3\text{O}_4@\text{GAC}$) particle electrodes for removal of furfural from aqueous solution. The particle electrodes structural and morphological featured were determined via BET, VSM, XRD, FE-SEM and FTIR techniques. The experiments were performed based on central composite design (CCD) and the role of influencing factors including reaction time, pH, voltage and initial furfural concentrations at five levels were evaluated. The Quadratic model with high correlation coefficient = 0.9872 (R^2 and $R_{\text{Adj}}^2 = 0.9724$) was suggested for experimental data analysis. The performance of electrochemical oxidation towards furfural degradation was enhanced substantially after adding $\text{Fe}_3\text{O}_4@\text{GAC}$. The highest furfural removal efficiency (98.2%) was achieved under optimal conditions (furfural: 201 mg/L, electrolysis time: 69 min, voltage: 19 V, and pH: 5.0). Besides, over 78 and 74 % of COD and TOC were removed by

* Corresponding authors at: Department of Environmental Health Engineering, School of Public Health, Ardabil University of Medical Sciences, Ardabil, Iran.

E-mail addresses: yusef.poureshgh@gmail.com (Y. Poureshgh), kakavandibvch@gmail.com (B. Kakavandi).

Peer review under responsibility of King Saud University.



Fe_3O_4 @GAC-based three-dimensional process, respectively. Based on the COD/TOC ratio and average oxidation state (AOS) index, a significant increase was observed in the biodegradability of intermediates of furfural after treatment. Results showed that three-dimensional electrochemical process with particle electrodes is a promising technology for efficient removal of furfural, even at high concentrations. Results of Liquid chromatography–mass spectrometry (LC-MS) analysis and degradation pathway showed that furfural could be oxidized to compounds with smaller molecular masses, which eventually converted to carbon dioxide and water.

© 2022 The Authors. Published by Elsevier B.V. on behalf of King Saud University. This is an open access article under the CC BY-NC-ND license (<http://creativecommons.org/licenses/by-nc-nd/4.0/>).

1. Introduction

Over the recent decades, an increase in the loads of contaminants in environmental resources has attracted the attention of researchers to devise new schemes for addressing the crisis (Dargahi et al., 2021; Samarghandi et al., 2020). Furfural, as an organic by-product and solvent from oil and petrochemical industries, paper and cardboard manufacturing has been widely observed in the effluents (Açıkıldız et al., 2014). The furfural concentrations in the effluents of such industries are reported to be in the range of 100–1200 mg/L (Li et al., 2016). Furfural, which is effective in removal of sulfur and oxygen, has been considered as a primary substance of furfural alcohol and tetrahydrofuran, and employed in production of resin and organic solvents. In addition, furfural has been used as an intermediate in production of different herbicides, fungicide and aromatics (Singh et al., 2009). Human exposure to furfural can occur through three main pathways including inhalation, ingestion, skin and eye contact. Exposure to furfural causes headache, red eyes, tears and pulmonary edema (Mao et al., 2012; Sahu et al., 2008). Furfural is stable at room temperature and chemically converts to CO and CO_2 at high temperatures. The volatility temperature for this chemical is 162 °C and the solubility in water is close to 83 g/L (Anbia and Mohammadi, 2009). According to the serious concerns of furfural to the environmental resources and human health, it is required to be separated from contaminated wastewater before discharging into the environment.

To date, various technologies such as biological treatments (Malibo et al., 2021), adsorption (Sahu et al., 2008; Abukhadra and Mohamed, 2019), advanced oxidation processes (AOPs) (González et al., 2021), and nanofiltration (Qi et al., 2011) have been applied for removing furfural from aquatic environments. However, each technique has shown either practical or economic limitations. For instance, the main disadvantages of biological methods are toxic effects of high furfural concentrations, being expensive, time consuming, being applicable only on a small scale and ultimately poor process efficiency (Faramarzpour et al., 2009). In addition, there are some disadvantages for adsorption process including preparation of the efficient adsorbents and regeneration of used adsorbents (Li et al., 2020). Over the recent years, AOPs, especially electrochemical methods, have become more popular for effective wastewater treatment, due, principally to, the increased production of effluents and their discharge into the environment (Zaroual et al., 2006; Kadji et al., 2022; Assassi et al., 2021). The electrochemical treatment has embraced over the recent years thanks to numerous advantages, including high efficiency in removal of different gaseous, liquid, and solid pollutants,

easy operation, simple equipment, low sludge production with low residence time and density, and environmentally friendly (Rajeshwar et al., 1994; Madi-Azegagh et al., 2019).

Electrochemical is also known as green chemistry. Despite these advantages, two-dimensional electrochemical methods have some disadvantages including short life of electrode materials and increasing the temperature during the treatment process (Kadji et al., 2021). To overcome these drawbacks, a three-dimensional electrochemical process can be employed via addition of some materials such as granular activated carbon (GAC), carbon aerogel (Açıkıldız et al., 2014), ceramic (Zhang et al., 2020), and kaolin as the particle electrodes. Among the mentioned materials, GAC has been mostly used to remove contaminants, due to the high surface to volume ratio and wide pore structures (Zhang et al., 2013). However, the main issue imposed for using GAC is the difficulties in recovery and separation from the solution, which needs filtration. Introduction of metal oxides with magnetic properties (e.g., CoFe_2O_4 , Fe_2O_3 , Fe_3O_4 , FeOH and etc.) into the GAC surfaces can be considered as an excellent approach to overcome these problems. Among these metal oxides, magnetite nanoparticles (Fe_3O_4) have been widely applied for magnetization of materials owing to the high magnetic intensity, simple preparation and significant catalytic activity in catalyst-based oxidation processes (Aissani et al., 2020). Hence, the presence of Fe_3O_4 -based materials in the electrochemical process enhances the decontamination efficiency thereby the efficient role of Fe ions in catalyzing the formed oxidant and subsequently the generation of additional reactive oxidizing species.

Response surface methodology (RSM), which is one of the effective methods for designing the experimental conditions, is a statistical technique based on the fit of a polynomial equation to the experimental data that must define the behavior of a data set with the objective of making statistical previsions. It can be well applied when a response or a set of responses of interest are influenced by several variables. The objective is to simultaneously optimize the levels of these variables to attain the best system performance (Afshin et al., 2020).

Many studies have been conducted in field of three-dimensional electrochemical with different particle electrodes. However, no study has done to evaluate the efficiency three-dimensional electrochemical process with Fe_3O_4 @GAC particle electrodes for removal of non-biodegradable pollutants such as furfural and evaluation of metabolites produced by furfural degradation by this process, which can be considered the main novelty of this study. Therefore, the aim of this study was to study the efficiency of the three-dimensional electrochemical process with Fe_3O_4 @GAC particle electrodes as the third dimension to remove furfural from aqueous solutions.

According to this description, the present study focuses on the fabrication of $\text{Fe}_3\text{O}_4@\text{GAC}$ magnetic and the investigation of its application and activity in three-dimensional electrochemical process towards degradation and mineralization of furfural for the first time. To the best of our knowledge, there is little information on the performance and the reaction mechanism of $\text{Fe}_3\text{O}_4@\text{GAC}$ -based three-dimensional electrochemical process to degrade furfural in the literature. The effect of some operating factors (e.g., solution pH, voltage, electrolysis time and initial furfural concentration) on electrode performance was evaluated and optimized by the RSM. After optimization, the mineralization and biodegradability studies were performed. Furthermore, the reaction mechanism of process as well as possible degradation pathway of furfural were described in details.

2. Materials and methods

2.1. Chemicals

In this study, all chemicals were applied without extra purification. Furfural (%98), granular activated carbon (GAC, 4–8 mesh and with a length of 2.36–4.75 mm), $\text{FeCl}_3 \cdot 6\text{H}_2\text{O}$ (% 97), $\text{FeCl}_2 \cdot 4\text{H}_2\text{O}$ (%98), sulfuric acid (H_2SO_4 , 0.1 M), sodium hydroxide (NaOH, 0.1 M) and ammonia solution (NH_4OH , 25%) were provided from Merck company (Germany). Moreover, deionized distilled water (DDW) was employed for preparation of solutions in whole the catalyst synthesis and environmental tests.

The response surface methodology (RSM) with least number of experimental experiments is a powerful tool for statistical modeling (Cojocar and Zakrzewska-Trznadel, 2007; Yahiaoui et al., 2010; Yahiaoui et al., 2011). RSM is a mathematical procedure based on nonlinear multivariate that consists of an experimental design to provide sufficient and reliable response values. RSM fits the information obtained from the experimental design and determine the optimal amount of independent variables at the desired response value (Montgomery, 2008; Assassi et al., 2021).

2.2. Preparation of $\text{Fe}_3\text{O}_4@\text{GAC}$ composites

Herein, firstly, Fe_3O_4 magnetite nanoparticles were synthesized through chemical co-precipitation method. In this regard, 5.4 g $\text{FeCl}_3 \cdot 6\text{H}_2\text{O}$ and 2.78 g $\text{FeCl}_2 \cdot 4\text{H}_2\text{O}$ (2:1 ratio, by weight) were mixed in 100 mL of DDW in a round bottom balloon at N_2 atmosphere. Then, 25 % ammonia solution was added in dropwise until the pH of solution reached 9.0 under strong stirring for 60 min at 75 °C. Finally, a black precipitate (i.e., Fe_3O_4 nanoparticles) was appeared, separated from reaction solution, and then washed with DDW and methanol for several times. For synthesis of $\text{Fe}_3\text{O}_4@\text{GAC}$, 22.4 g GAC was added to 200 mL DDW and mixed to ensure the homogenize state in an ultrasonic apparatus for 15 min. Then, 9.0 g Fe_3O_4 nanoparticles were added to the above solution and mixed for 15 min at 70 °C under a mechanical stirrer. The resulting particle electrode was collected from supernatant by a 1.3 Tesla magnet, washed several times with DDW, and finally dried at 70 °C for 12 h (Afshin et al., 2020; D'Cruz et al., 2020).

2.3. Characterization analyses

The crystallographic structure of as-prepared samples was characterized by X-ray diffraction (XRD) analysis (Philips PNA-analytical diffractometer) with diffractograms of $2\theta = 10\text{--}80^\circ$. The functional groups and chemical structure of samples were determined by Fourier transform infrared spectroscopy (FTIR, model FTS-165, BIO-RAD, USA) technique in spectral range of 400–4000 cm^{-1} . The surface morphology and structure of as-obtained magnetic nano-sized composite were characterized via field emission scanning electron microscopy (FE-SEM) (model Mira 3-XMU) at 10 keV. The magnetic properties of samples were measured using a vibrating sample magnetometer (VSM, (model 7400, Lake-share, USA).

2.4. Experimental procedure

Batch experiments were carried out in a laboratory scale. The equipment used for the electrolysis unit consisted of a rectangular glass chamber with an effective volume of 500 mL. Graphite anode and steel cathode electrodes (130 × 4 × 90 mm) were placed in the reactor. The power supply (model Adak, ps_405, Hamadan Kit CO, Iran) was used to provide energy. The schematic diagram of reactor is shown in Fig. 1. The electrodes were placed vertically and in parallel at a gap distance of 4 cm. To provide the third dimension of the 3D electrode, the space between the two electrodes was filled by the $\text{Fe}_3\text{O}_4@\text{GAC}$ composites with a constant concentration of 8 gr/500 mL. Due to the special characteristics of the reactor, the $\text{Fe}_3\text{O}_4@\text{GAC}$ composites was floated between the two electrodes. The magnetic stirrer with 250 rpm was employed to homogenize the solution within experiments. Different concentrations of furfural (mg/L) were obtained from the stock solution. The aliquot samples were withdrawn from different experimental conditions and centrifuged at 5000 rpm, and then filtered using a 0.22 μ filter to separate the impurities. The residual concentration of furfural was determined by a spectrophotometer (model DR5000 made by HACK) at wavelength of 275 nm (Sahu et al., 2008). To study of the mineralization degree, the chemical oxygen demand (COD) and total organic carbon (TOC) were determined by titration method (Sözen et al., 2020) and a TOC analyzer (Shimadzu-CSH E200), respectively. The removal efficiency of furfural in different experimental conditions were calculated according to Eq. (1):

$$\text{Removal efficiency}(\%) = \frac{C_0 - C_e}{C_0} \quad (1)$$

where, C_e and C_0 are the initial and final concentrations of furfural (mg/L), respectively.

Furthermore, the determination of intermediates of Furfural degradation was done by Liquid Chromatography - Tandem Mass Spectrometry (LC-MS) using a Waters Alliance 2695 HPLC-Micromass Quattro micro API Mass Spectrometer fitted with a Atlantis T3-C18 column (3 μm , 2.1 × 100 mm) at ambient temperature, with injection volume of 20 μL and flow rate of 0.25 mL/min. The mobile phase was a mixture of 60% acetonitrile + 0.1 % formic acid and 40 % water + 0.1 % formic acid.

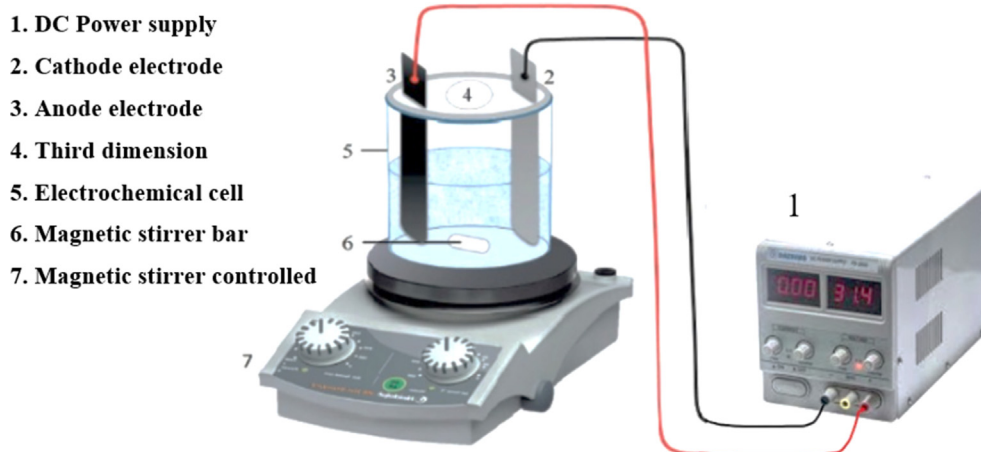


Fig. 1 A schematic representation of used three-dimensional electrochemical reactor in this study.

2.5. Experimental design (CCD) and mathematical models

In addition the actual values of operational parameters in each set of experiments are listed in [Table 1](#). Based on this design, 32 tests were set for modeling of the furfural removal by $\text{Fe}_3\text{O}_4@\text{GAC}$ -based three-dimensional electrochemical process to degrade furfural. In this regard, the effect of four independent factors: solution pH, electrolysis time, initial furfural concentrations and voltage at five levels ($+\alpha$, $+1$, 0 , -1 , $-\alpha$) was designed and evaluated. In addition the \times of the furfural removal by $\text{Fe}_3\text{O}_4@\text{GAC}$ -based three-dimensional electrochemical process as summarized in [Table 2](#). Furfural removal efficiency (Y) was defined as the response of the system. Herein, the actual values of the factors (X_i) were coded by Eq. (2) to compare various factors with different units.

$$A_i = \frac{X_i - X_0}{\Delta x} \quad (2)$$

where, A_i and X_0 are the coded and medium values of the factors, and Δx is the difference between the high and the median values of the factor.

3. Results and discussion

3.1. Structure characteristics of particular electrodes

[Fig. 2\(a\)](#) presents the XRD spectrum of particular electrodes. Three distinctive peaks located at 22.31° , 25.50° and 28.50° corresponding to carbon element in activated carbon structure ([Xu et al., 2017](#)). In addition, the peaks placed on 31.70° , 34.40° , 36.20° , 38.70° , 47.60° , 48.90° , and 56.50° prove the pres-

ence of iron oxide particles in the structure of Fe_3O_4 . Generally, the XRD analysis indicated that iron particles are successfully synthesized and doped on activated carbon ([Abdollahzadeh et al., 2020](#); [Gupta and Nayak, 2012](#)). [Fig. 2 \(b\)](#) shows the functional groups of $\text{Fe}_3\text{O}_4/\text{GAC}$ nanocomposite in the range of $400\text{--}4000\text{ cm}^{-1}$. As shown, several adsorption bands were observed at 3833 , 3732 , 3615 , 2360 , 2343 , 1540 , 1076 , 669 , 577 , and 419 cm^{-1} . The peaks at 3383 cm^{-1} are assigned to O-H, and peak at 3732 cm^{-1} corresponded to C = C. Furthermore, two peaks at 3615 and 2360 cm^{-1} are assigned to C-O. Peaks at 2343 cm^{-1} belong to functional group C-H ([Jiang et al., 2013](#); [Chieng et al., 2015](#)). In addition, peaks observed at 1540 , 1076 , 669 , 577 , 419 cm^{-1} are assigned to be for functional group Fe-O ([Pavan et al., 2014](#)).

[Fig. 3\(a-b\)](#) show the morphology and structure of GAC and $\text{Fe}_3\text{O}_4@\text{GAC}$. The uniform morphology of spherical particles of as-prepared Fe_3O_4 is clear in [Fig. 3\(a\)](#). The particle size distribution was determined to be approximately 17 nm in size ([Duman et al., 2016](#)). [Fig. 3\(b\)](#) displays that a number of Fe_3O_4 nanoparticles tends to combine with GAC which justifies the agglomeration of clusters. The white particles shown in [Fig. 3\(b\)](#) on the GAC prove the presence of Fe_3O_4 on the surfaces of particle electrode ([Yang et al., 2018](#)). Results of Energy Dispersive X-Ray Analysis (EDX) for $\text{GAC}@\text{Fe}_3\text{O}_4$ are shown in [Fig. 3\(c\)](#). EDX analysis was used to find the percentage of elements in nanoparticles and the percentage of output. Results showed that the $\text{GAC}@\text{Fe}_3\text{O}_4$ particles contained carbon (9.3%), oxygen (26.8%) and iron (64%). These results indicate that carbon has been added to the nanoparticle structure ([Takmil et al., 2020](#)).

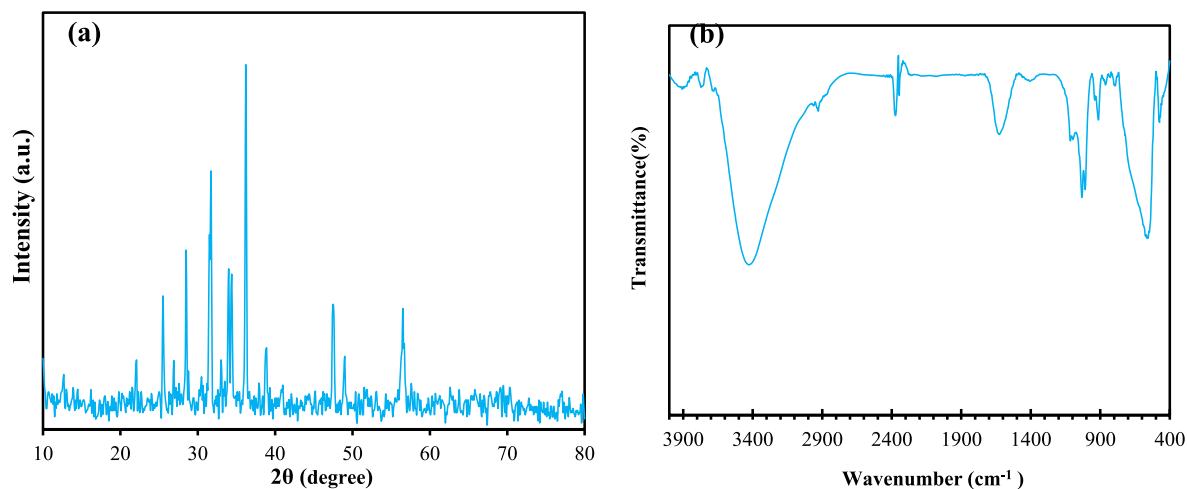
Results of Brunauer-Emmett-Teller analysis (BET) are shown in [Fig. 4\(a\)](#). Adsorbed and desorbed N_2 isotherms were

Table 1 Independent variables and their levels in the experimental design.

Independent variables	signs	the unit	$-\alpha$	-1	0	$+1$	$+\alpha$
pH	A	—	3	5	7	9	11
Voltage	B	V	5	10	15	20	25
Density	C	mg/L	100	200	300	400	500
Time	D	min	10	30	50	70	90

Table 2 CCD matrix along with observed and predicted response values for furfural removal using Fe₃O₄@GAC-based three-dimensional electrochemical process.

Run	Factor 1	Factor 2	Factor 3	Factor 4	Response 1	
	A:pH	B:VOL V	C:Conc mg/L	D:Time min	R1 %	Predicted Value
1	7	15	300	50	74.9	74.25
2	5	10	200	70	84.62	85.31
3	9	10	400	70	50.6	51.81
4	9	20	200	30	53.11	55.85
5	7	5	300	50	46.28	48.72
6	7	15	300	50	76.27	74.25
7	5	10	400	70	74.28	69.11
8	7	25	300	50	71.39	71.75
9	7	15	300	90	90.11	89.67
10	7	15	300	50	72.61	74.25
11	9	20	400	30	48.69	47.63
12	9	10	400	30	40.38	37.71
13	9	20	400	70	66.57	66.89
14	7	15	100	50	84.69	82.08
15	5	20	200	30	81.29	79.70
16	5	20	400	70	94.2	92.87
17	7	15	300	50	77.9	74.25
18	7	15	500	50	52.25	57.66
19	5	10	400	30	58.64	57.42
20	3	15	300	50	85.36	91.36
21	11	15	300	50	53.42	50.22
22	7	15	300	50	69.4	74.25
23	7	15	300	10	53.61	56.85
24	5	20	200	70	98.17	98.42
25	5	10	200	30	74.51	71.76
26	7	15	300	50	78.1	74.25
27	9	10	200	70	71.29	72.55
28	9	20	200	70	76.14	76.99
29	5	20	400	30	79.7	76.01
30	9	10	200	30	55.62	56.58
31	7	15	300	50	71.86	74.25
32	7	15	300	50	72.96	74.25

**Fig. 2** XRD pattern (a) and FTIR analysis (b) of the as-prepared GAC@Fe₃O₄.

analyzed for particular electrodes Fe₃O₄@GAC and GAC. The adsorption isotherm fit with IV and indicates the porosity of the particulate electrode Fe₃O₄@GAC and AC. As summa-

rized in Table 3, the specific surface area of GAC and Fe₃O₄@GAC were estimated to be 421.36 and 498.43 m²/g, respectively. In addition, the total pore volume in Fe₃O₄@-

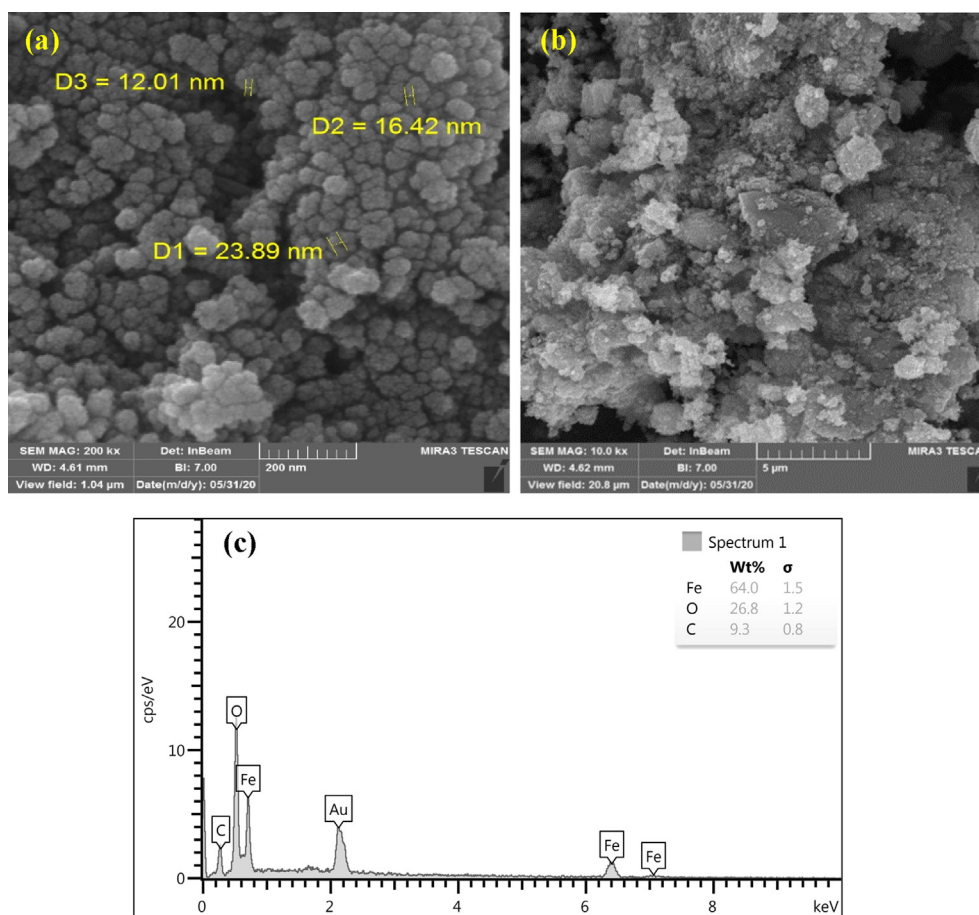


Fig. 3 FE-SEM images of Fe_3O_4 (a) and $\text{GAC}@Fe_3\text{O}_4$ (b); EDX analysis of $\text{GAC}@Fe_3\text{O}_4$.

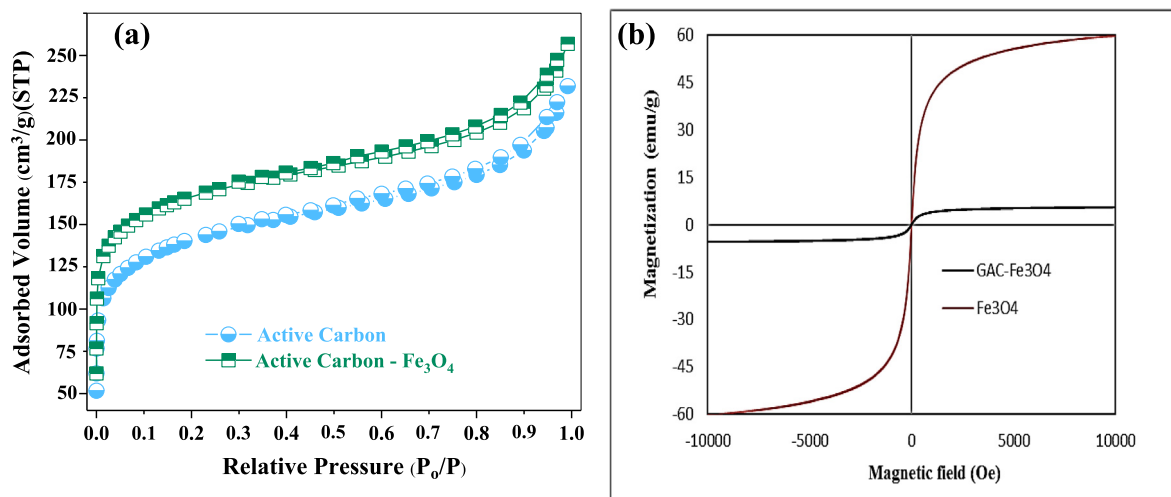


Fig. 4 N_2 adsorption-desorption isotherm of $\text{GAC}@Fe_3\text{O}_4$ (a) and magnetization curves of the as-prepared samples.

Table 3 The textural properties of GAC and $\text{Fe}_3\text{O}_4@\text{GAC}$.

Material	S_{BET} (m^2g^{-1})	S_{micro} (m^2g^{-1})	S_{meso} (m^2g^{-1})	V_{Total} (cm^3g^{-1})	V_{micro} (cm^3g^{-1})	V_{meso} (cm^3g^{-1})	D_p
GAC	421.36	251.65	169.71	0.4237	0.1256	0.2981	2.48
$\text{Fe}_3\text{O}_4@\text{GAC}$	498.43	289.62	208.81	0.4844	0.1410	0.3434	2.51

GAC and GAC particle electrodes were found to be 0.2981 and 0.3434 m³/g, respectively, which indicate the large pore volume in the particle electrode. Results of VSM analysis for Fe₃O₄@GAC are illustrated in Fig. 4(b). As observed, the particle electrodes are magnetic at room temperature and no hysteresis rings are observed in them. The magnetic saturation of pure Fe₃O₄ and Fe₃O₄@GAC particles were found to be 59.48 and 7.36 m²/g, respectively. A lower magnetic saturation for Fe₃O₄@GAC compared to pure Fe₃O₄ might be originated from the presence of non-magnetic GAC in the structure of Fe₃O₄@GAC particles. However, the Fe₃O₄@GAC particles can still be adsorbed rapidly to the external magnet, indicating a good magnetic response. Therefore, it can be concluded that the particle electrode employed in present study possess a good magnetic property which can be separated easily from the reaction mixture.

3.2. Development of regression model

CCD procedure was designed to estimate the actual and predicted values. As summarized in Table 2, a good relationship was observed between the predicted and experimental values. The quadratic polynomial model was the most suitable tool for optimization of furfural removal over Fe₃O₄@GAC-based three-dimensional electrochemical process. The regression coefficients (R² and R² adjusted) obtained from quadratic polynomial model suggest the high ability of model to fit the data obtained from furfural removal by electrochemical process. The empirical relationship between input and response variables based on coded values from CCD procedure is presented in Eq. (3).

$$Y = +38.01448 + 2.08260A + 4.63112B - 0.023877C + 0.242656D - 0.216812AB - 0.005672AC + 0.015109AD + 0.005324BC + 0.012906BD \quad (3)$$

where, Y represents the removal efficiency of furfural (%), as a response, A, B, C and D refer to solution pH, voltage, initial furfural concentration and reaction time, respectively.

According to Table 4, results of ANOVA analysis depict that the suggested model is statistically significant with linear conditions (P-value < 0.001). In addition, A, B, C and D parameters and interaction B² were found to be significant (p ≤ 0.001). The F value for this model was obtained 66.32, which indicates that the variance of each variable is more significant than the error variance and all main parameters play an important role as the response. F-Values showed that the effect of different parameters on the process follows in sequence: Initial furfural concentration < voltage < pH < reaction time.

According to the obtained results, solution pH with F = 179.9 is the most effective factor in the furfural oxidation process. In addition, the obtained adjusted correlation coefficient (R² (adj)) 0.9724 indicates the high accuracy of the statistical model. Fig. 5(a) shows the effect of effective variables on furfural oxidation (including pH, initial furfural concentration, voltage and reaction time). The range and selective range of variables, the degree of impact and the optimal points of each variable can be seen in this figure. According to the results of Pareto diagram, the effect of pH on furfural removal is more important than the other studied factors (see Fig. 5(b)),

followed by the initial furfural concentration, the reaction time and the next voltage.

3.3. Adequacy and validity of proposed model

Herein, various analyses were performed to validate the proposed model. The desirability and adequacy of the developed model were evaluated by plotting the predicted versus actual data and the studentized residuals versus predicted data are illustrated in Fig. 6. In the normal distribution (Fig. 6(b)), the data points are very close to each other and follow a straight descending line, indicating that the results obtained from the furfural removal fit well with a reasonable normal distribution. From Fig. 6(b) (the normal plot of residuals of furfural removal), it can be concluded that the data points are fairly close to the straight line, implying that the errors have a normal distribution with a zero mean and a constant value. The adequate adequacy measures the signal-to-noise ratio; where the ratio > 4 is desirable. A sufficient value of 23.531 was obtained from the present research, which shows justification the models for the process. The statistical Durbin-Watson test was used to detect the lack of correlation in the residual values of the proposed model. When the Durbin-Watson value reaches zero, there is a strong correlation between the regression residues. Alternatively, when Durbin-Watson value converges to 2, it can be postulated that there is a poor correlation or random distribution between successive points (Shokoohi et al., 2018). Durbin-Watson value in our experiment was estimated to be 2.18577. Generally, these results confirm that the proposed model sufficiently depicts the removal of furfural by Fe₃O₄@GAC-based three-dimensional electrochemical process.

3.4. The effect of key operating parameters

The influence of solution pH (Açıkyıldız et al., 2014; Li et al., 2016; Singh et al., 2009; Mao et al., 2012; Sahu et al., 2008; Anbia and Mohammadi, 2009; Malibo et al., 2021; Abukhadra and Mohamed, 2019; González et al., 2021) on the furfural removal efficiency is shown in Fig. 7 (a). The results showed that with increasing the pH, the furfural removal efficiency decreased. In general, the removal efficiency of furfural in pH = 5.0 experienced more stable than at the other pH values. As pH was either increased or decreased, the solution experienced the instability, which indicates the influence of the oxidation mechanisms and therefore the efficiency of furfural oxidation. The solution pH can affect the stability of the furfural structure and its concentration in solution; furfural is an intermediate compound of alcoholic and acidic compounds which can be influenced by solution pH (Mohsennejad et al., 2020). The solution pH has an effect on the structure of the studied pollutant, the mechanism of hydroxyl radical production, the reaction path and kinetics of the reactants (Dargahi et al., 2021). In addition, pH plays an important role in advanced oxidation processes, including electrochemical methods (Ben et al., 2009). At low pH values, there is a favorable situation for the production of OH[•] radicals, and these radicals are known with the higher potential for the degradation of pollutants, including furfural in an acidic environment (Molla Mahmoudi et al., 2020). Results obtained from the present research are inconsistent with Cai

Table 4 Analysis of variance of operational parameters in furfural elimination over $\text{Fe}_3\text{O}_4@\text{GAC}$ -based three-dimensional electrochemical process.

Source	Sum of Squares	df	Mean Square	F-value	p-value	
Model	6483.05	14	463.08	32.78	< 0.0001	significant
A-pH	2539.78	1	2539.78	179.79	< 0.0001	
B-VOL	795.23	1	795.23	56.29	< 0.0001	
C-Conc	895.12	1	895.12	63.36	< 0.0001	
D-Time	1615.89	1	1615.89	114.39	< 0.0001	
AB	75.21	1	75.21	5.32	0.0339	
AC	20.59	1	20.59	1.46	0.2439	
AD	5.84	1	5.84	0.4137	0.5287	
BC	113.37	1	113.37	8.03	0.0115	
BD	26.65	1	26.65	1.89	0.1874	
CD	3.47	1	3.47	0.2456	0.6266	
A ²	22.11	1	22.11	1.56	0.2279	
B ²	362.64	1	362.64	25.67	< 0.0001	
C ²	35.42	1	35.42	2.51	0.1317	
D ²	1.81	1	1.81	0.1282	0.7247	
Residual	240.15	17	14.13			
Lack of Fit	173.91	10	17.39	1.84	0.2160	not significant
Pure Error	66.24	7	9.46			
Cor Total	6723.20	31				

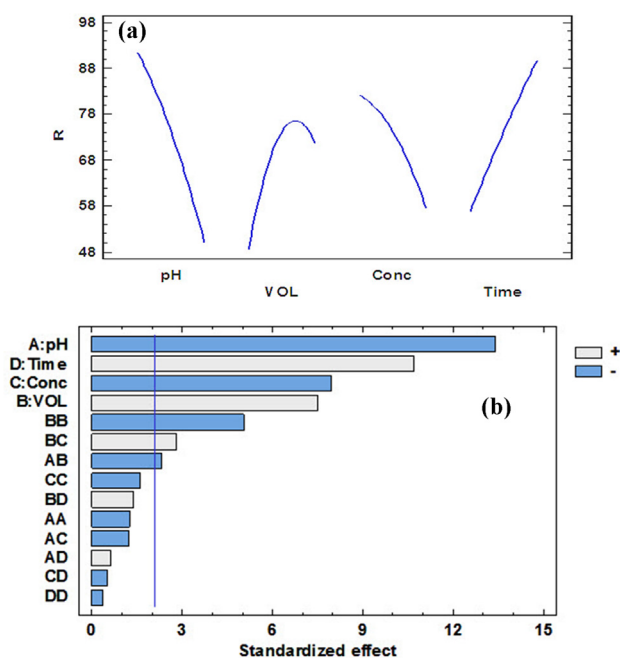


Fig. 5 The Pareto diagram for determination the influence of different variables on furfural removal efficiency by $\text{Fe}_3\text{O}_4@\text{GAC}$ -based three-dimensional electrochemical process (a) and the importance of the effects of influencing parameters on the performance of $\text{Fe}_3\text{O}_4@\text{GAC}$ -based three-dimensional electrochemical process (b).

et al. (Cai et al., 2018) and Liang, Su H-W (Liang and Su, 2009).

The effects of voltage on furfural removal efficiency are shown in Fig. 7(a). Accordingly, as the voltage increased from 5.0 to 20 V, the efficiency showed an increasing trend. However, further increase in the voltage from 20 to 25 V led to the reduction in the removal efficiency of furfural. According

to the results obtained from the present research, voltage 19 V was considered as the optimal value. The degradation process in the three-dimensional electrochemical system is directly related to the current density of the system, while the current density is proportional to the applied voltage. Therefore, the applied voltage affects the furfural removal. When the applied voltage increases from 5 to 19 V, a significant increase in furfural removal is observed. The most possible reason of this observation is that increasing the applied voltage leads to more polarization of electrode particles which accordingly increases the process of oxidation and surface reduction potential (Wang et al., 2008; Jung et al., 2015). However, when the applied voltage increased to 25 V, the furfural removal was decreased. These results may be due to the fact that the high electrolytic voltage exacerbates adverse reactions, which in turn is not desirable for furfural removal (Cao et al., 2013). The excessive increase in voltage and electric current increases adverse reactions and lower the reactor efficiency (Kermani et al., 2019; Samarghandi et al., 2021). Therefore, the optimum voltage applied to our system was 19 V, which is in line with the literature (Zhang et al., 2019).

Fig. 7(b) shows the effects of electrolysis time (15–90 min) on furfural removal efficiency. As observed, the furfural removal efficiency increased with increasing electrolysis time from 15 to 90 min. Increasing the electrolysis time in many treatment methods can lead to the more contact between the contaminant molecules and the oxidizing agents, which in turn increases the removal efficiency. Results showed that there is a direct relationship between electrolysis time and furfural removal efficiency; in which an increase in the electrolysis time leads to in the enhancement of the amount of hydroxyl radical, which in turn increases the furfural removal efficiency via a three-dimensional electrochemical process (Souri et al., 2020; Dargahi et al., 2022). The optimal contact time for the furfural removal was obtained 69 min.

Fig. 7(b) shows the effect of initial furfural concentrations (100–500 mg/L) on furfural removal efficiency in the electrochemical process. The highest efficiency was obtained at

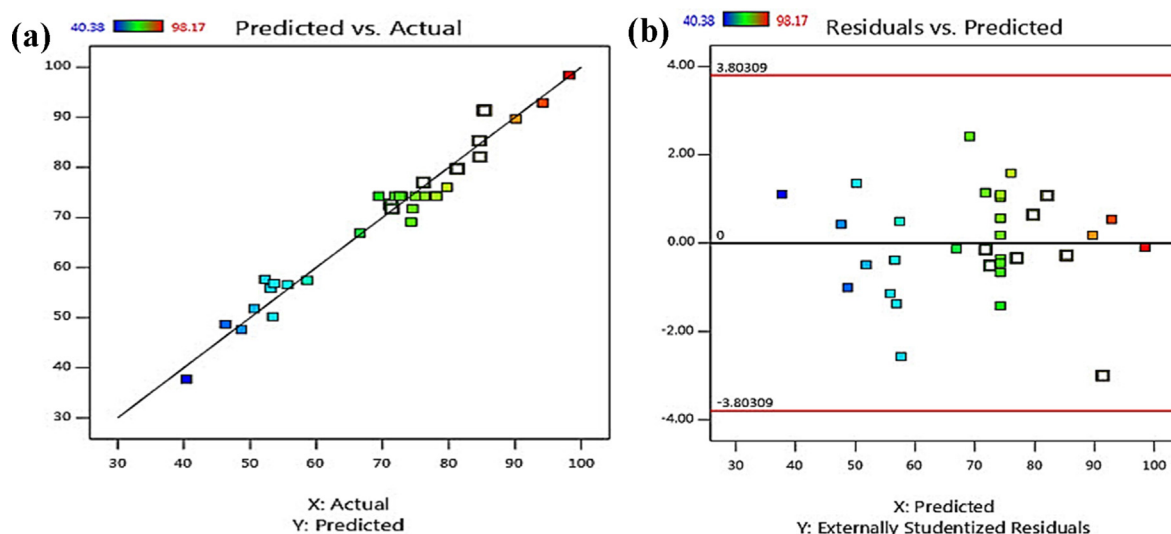


Fig. 6 The experimental data versus predicted data (a) and plots of studentized residuals versus predicted data for furfural by $\text{Fe}_3\text{O}_4@\text{GAC}$ -based three dimensional electrochemical process (b).

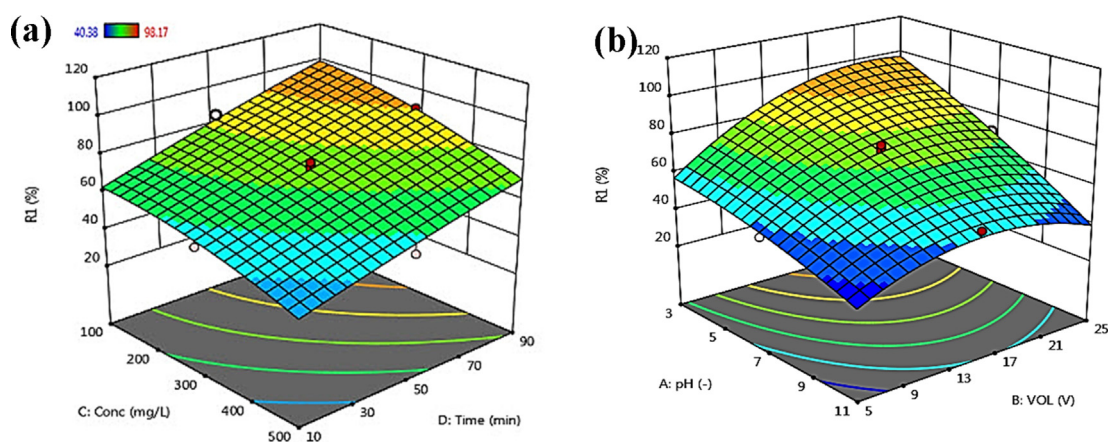


Fig. 7 The effects of operating parameters (a) voltage and solution pH; and (b) initial furfural concentration and reaction time on the efficiency of $\text{Fe}_3\text{O}_4@\text{GAC}$ -based three-dimensional electrochemical process.

Table 5 The performance of different processes towards furfural elimination.

Process	Furfural con. (mg/L or mM)	Reaction time (min)	Removal efficiency%	k_{obs} (min^{-1})	Ref.
ZnO-Mg nano photocatalyst	10 mg/L	60	89	0.004	(Mohsennejad et al., 2020)
Thermochemical activation of persulfate	84.3 mg/L	60	> 98.4	0.051	(Shokoohi et al., 2019)
UVC/ TiO_2 photocatalytic process	400 mg/L	300	98.3	0.0165	(Gholami et al., 2018)
heat-activated persulfate	–	120	90	< 0.018	(Manz et al., 2018)
NiS-clinoptilolite zeolite photocatalytic process	6 mM	120	80	0.006	(Nezamzadeh-Ejhieh and Moeinirad, 2011)
TiO_2 -coated perlite granules	0.6 mM	120	> % 95	0.022	(Faramarzpour et al., 2009)
heat-activated persulfate in the presence of nZVI-rGO catalyst	–	50	97.8	0.0842	(Rahmani et al., 2020)
three-dimensional electrochemical process with graphite anode	201 mg/L	70	98.20%	0.072	Present study

201 mg/L concentration. Since pollutants are observed with different concentrations in industries, it is necessary to study the effect of various pollutant concentrations on degradation efficiency (Yao et al., 2019; Rajkumar et al., 2018). Due to the fact that the number of reactive radicals produced in different concentrations is the same, the removal efficiency is expected to be different.

3.5. Process optimization using RSM

In this work, we used Design Expert 7.01 software with a multiple-response method to determine the optimum values of operational factors such as reaction time, voltage, initial furfural concentration and the solution pH for removal of furfural by electrochemical oxidation process. Under the optimum conditions (pH: 5.0, reaction time: 70 min, voltage: 19 V and initial furfural concentration: 201 mg/L), the highest furfural degradation was found to be 97.69 %, which was consistent with the values predicted by the software (98.22%). These results confirmed the model prediction for furfural degradation and were used as favorable conditions for further analysis and determination of the effect of other factors. An excellent correlation between the removal efficiencies of the observed and the predicted values demonstrated the high desirability of CCD approach.

Table 5 summarizes the performance of some oxidation processes towards furfural degradation, as reported in the literature. As can be seen, Fe₃O₄@GAC-based three-dimensional possess a better performance compared to other systems in the elimination of high concentrations of furfural. The difference in the efficiency of various processes may be associated to the differences in the operational factors, such as the type and quantity of catalyst, initial furfural concentration, reaction time, pH, type of process, and so forth. This comparison elucidated that the electrochemical degradation combined with Fe₃O₄@GAC can be introduced as an efficient and promising technique towards furfural degradation. Accordingly, electrochemical degradation with graphite anode can be employed as an alternative process to eliminate environmental pollutants, including non-petroleum pollutants.

3.6. Kinetic study

Kinetics is known as one of main steps to evaluate the decontamination rate of pollutant per time unite. In this work, the obtained experimental data from furfural degradation by Fe₃O₄@GAC-based electrochemical process under optimum conditions were described using pseudo-first-order kinetic model (Eq. (4)) as follows (Samarghandi et al., 2020):

$$k_{obs} = -\ln \frac{C}{C_0} \quad (4)$$

where, k_{obs} (min⁻¹), C_0 , and C are the apparent coefficient of degradation rate constant, initial furfural concentration, and furfural concentration after a certain time (t), respectively. A high value for regression coefficient ($R^2 > 0.93$) confirmed that the experimental data of the furfural degradation are in a good agreement with pseudo-first-order kinetic model (see Fig. 8(a)). The reaction rate constant was found to be 0.072 min⁻¹, which was greater than other studies with higher furfural concentration and less reaction time as illustrated in

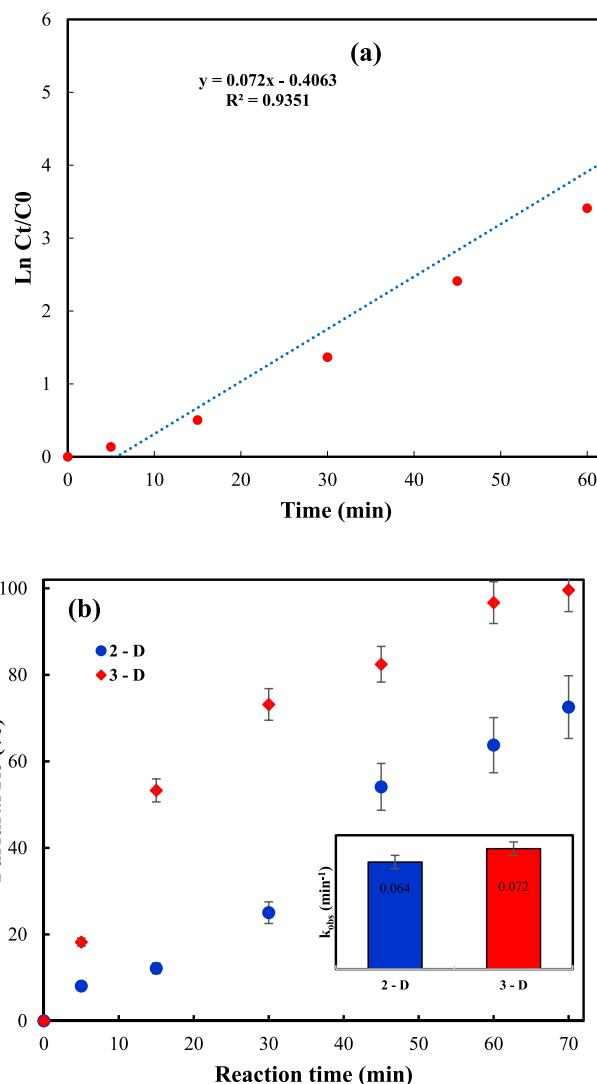


Fig. 8 (a) Pseudo-first-order kinetic for the degradation of furfural by Fe₃O₄@GAC-based three dimensional electrochemical process and the comparison between two-dimensional and three-dimensional processes towards furfural degradation under optimal conditions and the corresponding the reaction kinetics (insert) (pH: 5, reaction time: 90 min, voltage: 19 V and furfural concentration: 201 mg/L).

Table 5. Results of this study are consistent with previous studies on decontamination of organics over various electrochemical oxidation systems (Kong et al., 2006).

3.7. Oxidation rate in three-dimensional and two-dimensional electrochemical processes

It is well recognized that 3D electrochemical process is established based on 2D electrochemical process with many similarities such as electrode materials and treatment processes, except the third electrode. It is also named particle electrode or bed electrode, is basically granular or fragmental materials which are filled between two counter electrodes (Zhao et al., 2010; Martinez-Huitle and Ferro, 2006). The furfural degradation rate between the two-dimensional and Fe₃O₄@GAC-

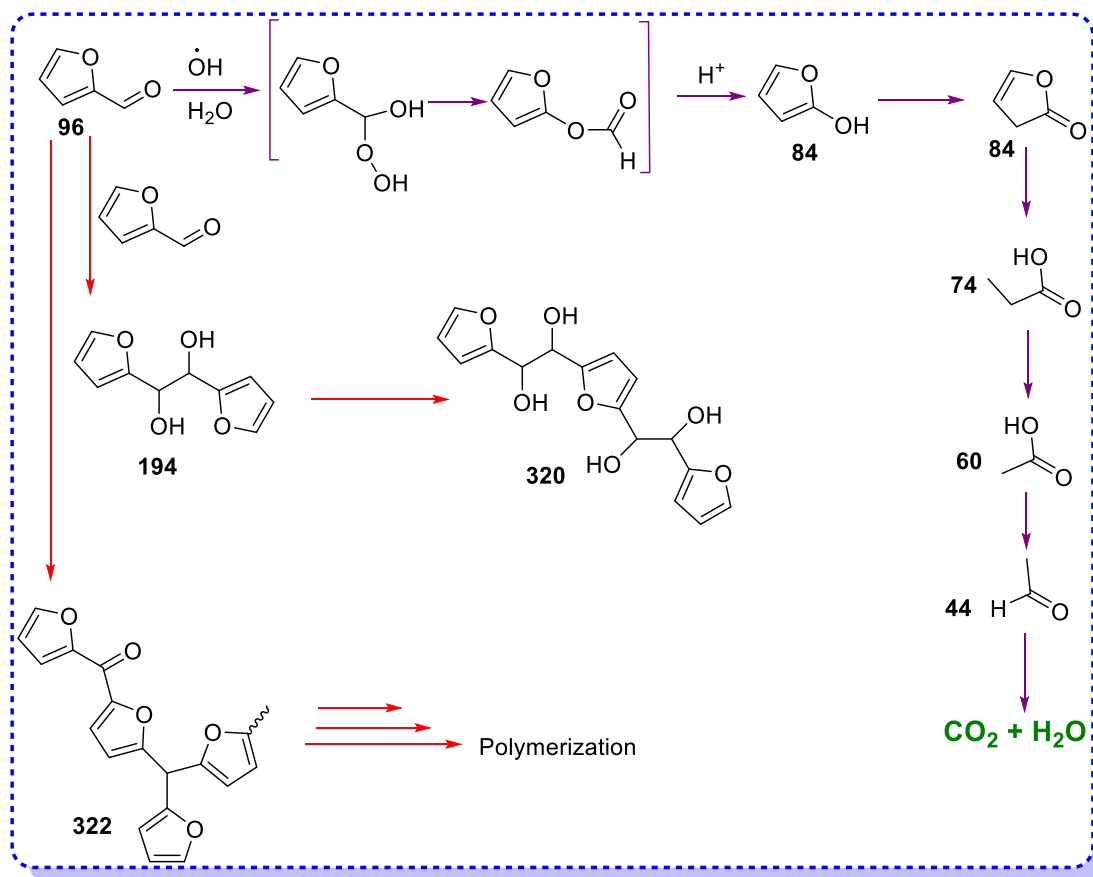


Fig. 9 Proposed pathways for furfural degradation during $\text{Fe}_3\text{O}_4@\text{GAC}$ -based three-dimensional electrochemical process.

based three-dimensional was compared under optimum conditions. As presented in Fig. 8(b), three-dimensional (3-D) process showed a better performance towards the elimination of furfural in comparison with two-dimensional (2-D) process. After 70 time reaction, the efficiencies of 99.6 and 72.5 % were achieved by 3-D and 2-D processes, respectively. Apart from higher removal efficiency, the reaction rate constant (k_{obs}) of three-dimensional process (0.065 min^{-1}) was greater than that of two-dimensional process (0.059 min^{-1}). The third dimension acts as a catalyst and increases the efficiency; the polar particles cause mass transfer between the furfural and the electrodes, which accelerates the furfural degradation at the electrode surface (Kong et al., 2006). It clearly verifies that the COD removal efficiency in 3D system is higher than that in 2D system, demonstrating the advantages of 3D system sufficiently (Zhang et al., 2013). Similar results have also been reported in the literature (Zhang et al., 2019).

3.8. Mineralization assessment

The mineralization is an index means breaking the C-C bonds of organic compounds to either smaller or simpler substances and ultimately CO_2 and H_2O . For this purpose, COD and TOC were employed as mineralization indices of furfural. Under the optimum conditions (pH: 5.0, V: 19 V, initial furfural concentration of 201 mg/L and reaction time 90 min), COD and TOC removal efficiencies by 3-D process were found to be 78.5 and 74.2 %, respectively, within 90 min reac-

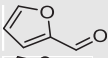
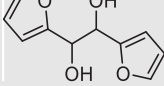
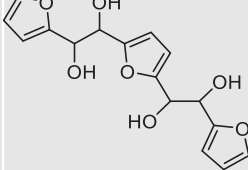
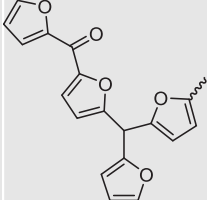
tion. These results demonstrated that $\text{Fe}_3\text{O}_4@\text{GAC}$ -based three-dimensional process is able to mineralize furfural which confirms the generation of various intermediates during the treatment process. In order to evaluate the biodegradability of effluent from furfural degradation by three-dimensional electrochemical process, the average oxidation state (AOS) and COD/TOC ratio were applied. The value of AOS can be calculated using Eq. (5) (Seidmohammadi et al., 2021). AOS varies between -4 as most reduced conditions and $+4$ as most oxidized conditions (Molla Mahmoudi et al., 2020; Dargahi et al., 2022; Seid-Mohammadi et al., 2020). It was found that with increasing the reaction time from 0 to 90 min, the AOS value witnessed an increasing trend from 1.01 to 1.51 and also the COD/TOC ratio decreased from 1.98 to 1.65. This observation suggests the generation of intermediate products with higher biodegradability during furfural degradation through $\text{Fe}_3\text{O}_4@\text{GAC}$ -based three-dimensional process.

$$\text{AOS} = 4 - 1.5 \frac{\text{COD}}{\text{TOC}} \quad (5)$$

3.9. Intermediates and degradation pathway

According to the results of LC-MS analysis, the degradation pathway of furfural in the $\text{Fe}_3\text{O}_4@\text{GAC}$ -based three-dimensional process is shown in Fig. 9. More information on the chemical structures and characterization of intermediates are summarized in Table 6. During electrochemical degrada-

Table 6 Intermediated identified by LC-MS in electrochemical degradation of furfural by anodic oxidation at graphite anode.

Structure	Molecular Weight	Iupac name
	96	furan-2-carbaldehyde
	84	furan-2-ol
	84	furan-2(3H)-one
	74	propionic acid
	60	acetic acid
	44	Acetaldehyde
	194	1,2-di(furan-2-yl)ethane-1,2-diol
	320	2,2'-(furan-2,5-diyl)bis(1-(furan-2-yl)ethane-1,2-diol)
	322	furan-2-yl(5-(furan-2-yl(5-methylfuran-2-yl)methyl)furan-2-yl)methanone

tion process, furfural can be oxidized to the compounds with smaller molecular masses. As reported in the literature (Malibo et al., 2021; Yang et al., 2021), furfural in the presence of an oxidizing agent such as a hydroxide radical converts to furan-2-ol or furan-2 (3H) -one compound with molecular mass of 84. Then, by opening the foramen ring (hydrolysis), various acids such as propionic acid, acetic acid and acetaldehyde are formed. Eventually, the resulting compound is converted to non-toxic compounds such as CO₂ and water. However, higher molecules in this mass spectrum may be related to the dimerization and polymerization processes after the oxidation process. Therefore, two furfural molecules can form International Union of Pure and Applied Chemistry (IUPACK) (1,2-di (furan-2-yl) ethane-1,2-diol) with a mass of 194. In addition, the polymerization pathway can produce heavier compounds such as furan-2-yl (5- (furan-2-yl (5-methylfuran-2-yl) methyl) furan-2-yl) methanone with a mass of 322.

3.10. Energy consumption

From the economic point of view, the energy consumption during the electrochemical degradation process is an important factor in practical applications. For this purpose, the electrical energy consumption during the degradation of furfural over

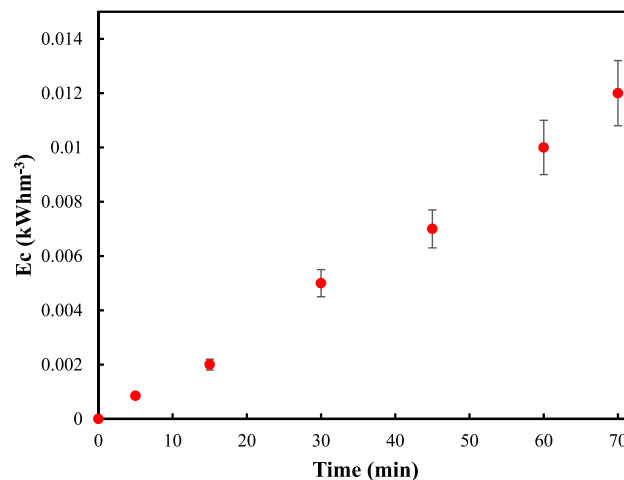


Fig. 10 Energy consumption in terms of voltage and constant current intensity during furfural degradation in Fe₃O₄@GAC-based three-dimensional electrochemical process.

Fe₃O₄@GAC-based three-dimensional process at different current densities was calculated using the following equation:

$$E = \frac{VI t_e}{V_s} \quad (6)$$

where, E is the electrical energy consumption (kWhm^{-3}), V is the applied voltage, I refers to the applied current (A), t_e is the electrolysis time (min) and V_s is the volume of the furfural solution (m^3). At higher current densities, energy consumption is increased which can be attributed to the increased evolution of hydrogen and oxygen. As represented in Fig. 10, the amount of energy consumption was found to be 0.011 kWhm^{-3} under optimum conditions.

4. Conclusion

The results obtained from the present study showed that the highest removal efficiencies of furfural, COD and TOC in electrochemical oxidation were found to be 98.22, 78.5 and 74.18%, respectively under optimum conditions (pH: 5.0, electrolysis time: 69 min, initial furfural concentration = 201 mg/L and voltage = 19 V). According to the analysis of variance (ANOVA) and the proposed quadratic model, current density and time are the most important positive parameters and pH and initial furfural concentrations are the most important negative parameters in the efficiency of the electrooxidation process. Results also indicated that increasing the applied current density and electrolysis time led to the enhancement of the furfural and COD removal efficiencies. While, furfural removal efficiency decreased as increase was observed in the initial furfural concentrations and solution pH. The furfural degradation fits the quasi-first-order kinetic model. According to the results obtained from the present study, it can be concluded that the electrochemical method with $\text{Fe}_3\text{O}_4@\text{GAC}$ can be used with high efficiency and less expenses for furfural oxidation. In addition, CCD method is an efficient way to reduce costs and experimental works, and the study of interactions between influential factors in the process can help us for better understanding of the effects of independent variables on the dependent variable.

Declaration of Competing Interest

The authors declare that they have no known competing financial interests or personal relationships that could have appeared to influence the work reported in this paper.

Acknowledgements

This study was financial supported by Ardabil University of Medical Sciences and Health Services, we gratefully acknowledge them. The protocol was approved by the Institutional Review Board of Ardabil University of Medical Sciences (Approval ID: IR.ARUMS.REC.1399.140).

References

- Abdollahzadeh, H., Fazlzadeh, M., Afshin, S., Arfaeinia, H., Feizizadeh, A., Poureshgh, Y., et al, 2020. Efficiency of activated carbon prepared from scrap tires magnetized by Fe_3O_4 nanoparticles: characterisation and its application for removal of reactive blue19 from aquatic solutions. *Int. J. Environ. Anal. Chem.* 1–15.
- Abukhadra, M.R., Mohamed, A.S., 2019. Adsorption removal of safranin dye contaminants from water using various types of natural zeolite. *Silicon*. 11 (3), 1635–1647.
- Açıkyıldız, M., Gürses, A., Karaca, S., 2014. Preparation and characterization of activated carbon from plant wastes with chemical activation. *Microporous Mesoporous Mater.* 198, 45–49.
- Afshin, S., Rashtbari, Y., Ramavandi, B., Fazlzadeh, M., Vosoughi, M., Mokhtari, S.A., et al, 2020. Magnetic nanocomposite of filamentous algae activated carbon for efficient elimination of cephalalexin from aqueous media. *Korean J. Chem. Eng.* 37 (1), 80–92.
- Aissani, T., Yahiaoui, I., Boudrahem, F., Yahia Cherif, L., Fourcad, F., Amrane, A., et al, 2020. Sulfamethazine degradation by heterogeneous photocatalysis with ZnO immobilized on a glass plate using the heat attachment method and its impact on the biodegradability. *Reaction kinetics, mechanisms and catalysis*. 131 (1), 471–487.
- Anbia, M., Mohammadi, N., 2009. A nanoporous adsorbent for removal of furfural from aqueous solutions. *Desalination* 249 (1), 150–153.
- Assassi, M., Madjene, F., Amrane, A., 2021. Degradation of an organophosphorus insecticide in aqueous medium by Electro-Fenton process. *Acta Periodica Technologica*. 52, 63–72.
- Assassi, M., Madjene, F., Harchouche, S., Boulfiza, H., 2021. Photocatalytic treatment of Crystal Violet in aqueous solution: Box-Behnken optimization and degradation mechanism. *Environ. Prog. Sustainable Energy* 40, (6) e13702.
- Ben, W., Qiang, Z., Pan, X., Chen, M., 2009. Removal of veterinary antibiotics from sequencing batch reactor (SBR) pretreated swine wastewater by Fenton's reagent. *Water Res.* 43 (17), 4392–4402.
- Cai, J., Zhou, M., Yang, W., Pan, Y., Lu, X., Serrano, K.G., 2018. Degradation and mechanism of 2, 4-dichlorophenoxyacetic acid (2, 4-D) by thermally activated persulfate oxidation. *Chemosphere* 212, 784–793.
- Cao, G., Xu, F., Xia, S., 2013. Preparation of a composite particle electrode by electroless plating and its electrocatalytic performance in the decolorization of methyl orange dye solution. *J. Braz. Chem. Soc.* 24 (12), 2050–2058.
- Chiang, H.I., Lim, L.B., Priyantha, N., 2015. Enhancing adsorption capacity of toxic malachite green dye through chemically modified breadnut peel: equilibrium, thermodynamics, kinetics and regeneration studies. *Environ. Technol.* 36 (1), 86–97.
- Cojocaru, C., Zakrzewska-Trznadel, G., 2007. Response surface modeling and optimization of copper removal from aqua solutions using polymer assisted ultrafiltration. *J. Membr. Sci.* 298 (1–2), 56–70.
- Dargahi, A., Hasani, K., Mokhtari, S.A., Vosoughi, M., Moradi, M., Vaziri, Y., 2021. Highly effective degradation of 2, 4-Dichlorophenoxyacetic acid herbicide in a three-dimensional sono-electro-Fenton (3D/SEF) system using powder activated carbon (PAC)/ Fe_3O_4 as magnetic particle electrode. *J. Environ. Chem. Eng.* 9, (5) 105889.
- Dargahi, A., Shokoohi, R., Asgari, G., Ansari, A., Nematollahi, D., Samarghandi, M.R., 2021. Moving-bed biofilm reactor combined with three-dimensional electrochemical pretreatment (MBBR-3DE) for 2, 4-D herbicide treatment: application for real wastewater, improvement of biodegradability. *RSC Adv.* 11 (16), 9608–9620.
- Dargahi, A., Vosoughi, M., Mokhtari, S.A., Vaziri, Y., Alighadri, M., 2022. Electrochemical degradation of 2, 4-Dinitrotoluene (DNT) from aqueous solutions using three-dimensional electrocatalytic reactor (3DER): Degradation pathway, evaluation of toxicity and optimization using RSM-CCD. *Arabian J. Chem.* 15, (3) 103648.
- Dargahi, A., Barzoki, H.R., Vosoughi, M., Mokhtari, S.A., 2022. Enhanced electrocatalytic degradation of 2, 4-Dinitrophenol (2, 4-DNP) in three-dimensional sono-electrochemical (3D/SEC) process equipped with $\text{Fe}/\text{SBA}-15$ nanocomposite particle electrodes: Degradation pathway and application for real wastewater. *Arabian J. Chem.* 15, (5) 103801.

- D'Cruz, B., Madkour, M., Amin, M.O., Al-Hetlani, E., 2020. Efficient and recoverable magnetic AC-Fe₃O₄ nanocomposite for rapid removal of promazine from wastewater. *Mater. Chem. Phys.* 240, 122109.
- Duman, O., Tunç, S., Polat, T.G., Bozoğlan, B.K., 2016. Synthesis of magnetic oxidized multiwalled carbon nanotube-κ-carrageenan-Fe₃O₄ nanocomposite adsorbent and its application in cationic Methylene Blue dye adsorption. *Carbohydr. Polym.* 147, 79–88.
- Faramarzpour, M., Vossoughi, M., Borghei, M., 2009. Photocatalytic degradation of furfural by titania nanoparticles in a floating-bed photoreactor. *Chem. Eng. J.* 146 (1), 79–85.
- Gholami, N., Ghasemi, B., Anvaripour, B., Jorfi, S., 2018. Enhanced photocatalytic degradation of furfural and a real wastewater using UVC/TiO₂ nanoparticles immobilized on white concrete in a fixed-bed reactor. *J. Ind. Eng. Chem.* 62, 291–301.
- González, C., Pariente, M.I., Molina, R., Masa, M.O., Espina, L.G., Melero, J.A., et al., 2021. Study of highly furfural-containing refinery wastewater streams using a conventional homogeneous Fenton process. *J. Environ. Chem. Eng.* 9, (1) 104894.
- Gupta, V., Nayak, A., 2012. Cadmium removal and recovery from aqueous solutions by novel adsorbents prepared from orange peel and Fe₂O₃ nanoparticles. *Chem. Eng. J.* 180, 81–90.
- Jiang, Y., Luo, Y., Zhang, F., Guo, L., Ni, L., 2013. Equilibrium and kinetic studies of CI Basic Blue 41 adsorption onto N, F-codoped flower-like TiO₂ microspheres. *Appl. Surf. Sci.* 273, 448–456.
- Jung, K.-W., Hwang, M.-J., Park, D.-S., Ahn, K.-H., 2015. Combining fluidized metal-impregnated granular activated carbon in three-dimensional electrocoagulation system: feasibility and optimization test of color and COD removal from real cotton textile wastewater. *Sep. Purif. Technol.* 146, 154–167.
- Kadji, H., Yahiaoui, I., Garti, Z., Amrane, A., Aissani-Benissad, F., 2021. Kinetic degradation of amoxicillin by using the electro-Fenton process in the presence of a graphite rods from used batteries. *Chin. J. Chem. Eng.* 32, 183–190.
- Kadji, H., Yahiaoui, I., Akkouche, F., Boudrahem, F., Ramdani, S., Saidane, A., et al., 2022. Heterogeneous degradation of amoxicillin in the presence of synthesized alginate-Fe beads catalyst by the electro-Fenton process using a graphite cathode recovered from used batteries. *Water Sci. Technol.* 85 (6), 1840–1854.
- Kermani, M., Mehralipour, J., Kakavandi, B., 2019. Photo-assisted electroperoxone of 2,4-dichlorophenoxy acetic acid herbicide: Kinetic, synergistic and optimization by response surface methodology. *J. Water Process Eng.* 32, 100971.
- Kong, W., Wang, B., Ma, H., Gu, L., 2006. Electrochemical treatment of anionic surfactants in synthetic wastewater with three-dimensional electrodes. *J. Hazard. Mater.* 137 (3), 1532–1537.
- Li, S., Tang, J., Liu, Q., Liu, X., Gao, B., 2020. A novel stabilized carbon-coated nZVI as heterogeneous persulfate catalyst for enhanced degradation of 4-chlorophenol. *Environ. Int.* 138, 105639.
- Li, Y., Wang, X., Shao, J., Li, P., Yang, H., Chen, H., 2016. Utilization of pyrolytic char derived from bamboo chips for furfural removal: Kinetics, isotherm, and thermodynamics. *Energy Sources Part A* 38 (11), 1520–1529.
- Liang, C., Su, H.-W., 2009. Identification of sulfate and hydroxyl radicals in thermally activated persulfate. *Ind. Eng. Chem. Res.* 48 (11), 5558–5562.
- Madi-Azegagh, K., Yahiaoui, I., Boudrahem, F., Aissani-Benissad, F., Vial, C., Audonnet, F., et al., 2019. Applied of central composite design for the optimization of removal yield of the ketoprofen (KTP) using electrocoagulation process. *Sep. Sci. Technol.* 54 (18), 3115–3127.
- Malibo, P.M., Makgwane, P.R., Baker, P.G.L., 2021. Hetero-mixed TiO₂-SnO₂ interfaced nano-oxide catalyst with enhanced activity for selective oxidation of furfural to maleic acid. *Inorg. Chem. Commun.* 129, 108637.
- Manz, K.E., Adams, T.J., Carter, K.E., 2018. Furfural degradation through heat-activated persulfate: Impacts of simulated brine and elevated pressures. *Chemical Engineering Journal.* 353, 727–735.
- Mao, L., Zhang, L., Gao, N., Li, A., 2012. FeCl₃ and acetic acid co-catalyzed hydrolysis of corncob for improving furfural production and lignin removal from residue. *Bioresour. Technol.* 123, 324–331.
- Martinez-Huitle, C.A., Ferro, S., 2006. Electrochemical oxidation of organic pollutants for the wastewater treatment: direct and indirect processes. *Chem. Soc. Rev.* 35 (12), 1324–1340.
- Mohsennejad, M., Rasouli, Y., Jahangiri, M., 2020. Modeling and kinetic study of furfural degradation through the chemical surface modification of zinc oxide nanoparticles by magnesium. *Chem. Eng. J.* 393, 124677.
- Molla Mahmoudi, M., Khaghani, R., Dargahi, A., Monazami, T.G., 2020. Electrochemical degradation of diazinon from aqueous media using graphite anode: Effect of parameters, mineralisation, reaction kinetic, degradation pathway and optimisation using central composite design. *Int. J. Environ. Anal. Chem.* 1–26.
- Montgomery, D., 2008. Design and analysis of experiments. John Wiley & Sons, Inc, New York.
- Nezamzadeh-Ejhi, A., Moeinirad, S., 2011. Heterogeneous photocatalytic degradation of furfural using NiS-clinoptilolite zeolite. *Desalination.* 273 (2–3), 248–257.
- Pavan, F.A., Camacho, E.S., Lima, E.C., Dotto, G.L., Branco, V.T., Dias, S.L., 2014. Formosa papaya seed powder (FPSP): preparation, characterization and application as an alternative adsorbent for the removal of crystal violet from aqueous phase. *J. Environ. Chem. Eng.* 2 (1), 230–238.
- Qi, B., Luo, J., Chen, X., Hang, X., Wan, Y., 2011. Separation of furfural from monosaccharides by nanofiltration. *Bioresour. Technol.* 102 (14), 7111–7118.
- Rahmani, A., Salari, M., Tari, K., Shabanloo, A., Shabanloo, N., Bajalan, S., 2020. Enhanced degradation of furfural by heat-activated persulfate/nZVI-rGO oxidation system: Degradation pathway and improving the biodegradability of oil refinery wastewater. *J. Environ. Chem. Eng.* 8, (6) 104468.
- Rajeshwar, K., Ibanez, J.G., Swain, G.M., 1994. Electrochemistry and the environment. *J. Appl. Electrochem.* 24 (11), 1077–1091.
- Rajkumar, C., Veerakumar, P., Chen, S.-M., Thirumalraj, B., Lin, K.-C., 2018. Ultrathin sulfur-doped graphitic carbon nitride nanosheets as metal-free catalyst for electrochemical sensing and catalytic removal of 4-nitrophenol. *ACS Sustainable Chem. Eng.* 6 (12), 16021–16031.
- Sahu, A.K., Srivastava, V.C., Mall, I.D., Lataye, D.H., 2008. Adsorption of furfural from aqueous solution onto activated carbon: Kinetic, equilibrium and thermodynamic study. *Sep. Sci. Technol.* 43 (5), 1239–1259.
- Samarghandi, M.R., Dargahi, A., Shabanloo, A., Nasab, H.Z., Vaziri, Y., Ansari, A., 2020. Electrochemical degradation of methylene blue dye using a graphite doped PbO₂ anode: optimization of operational parameters, degradation pathway and improving the biodegradability of textile wastewater. *Arabian J. Chem.* 13 (8), 6847–6864.
- Samarghandi, M.R., Ansari, A., Dargahi, A., Shabanloo, A., Nematollahi, D., Khazaei, M., et al., 2021. Enhanced electrocatalytic degradation of bisphenol A by graphite/β-PbO₂ anode in a three-dimensional electrochemical reactor. *J. Environ. Chem. Eng.* 9, (5) 106072.
- Samarghandi, M.R., Dargahi, A., Zolghadr Nasab, H., Ghahramani, E., Salehi, S., 2020. Degradation of azo dye Acid Red 14 (AR14) from aqueous solution using H₂O₂/nZVI and S₂O₈²⁻/nZVI processes in the presence of UV irradiation. *Water Environment Research* 92 (8), 1173–1183.
- Seid-Mohammadi, A., Ghorbanian, Z., Asgari, G., Dargahi, A., 2020. Photocatalytic degradation of metronidazole (MnZ) antibiotic in aqueous media using copper oxide nanoparticles activated by

- H₂O₂/UV process: Biodegradability and kinetic studies. *Desalin Water Treat.* 193, 369–380.
- Seidmohammadi, A., Vaziri, Y., Dargahi, A., Nasab, H.Z., 2021. Improved degradation of metronidazole in a heterogeneous photo-Fenton oxidation system with PAC/Fe₃O₄ magnetic catalyst: biodegradability, catalyst specifications, process optimization, and degradation pathway. *Biomass Convers. Biorefin.*, 1–17
- Shokoohi, R., Samadi, M.T., Amani, M., Poureshgh, Y., 2018. Optimizing laccase-mediated amoxicillin removal by the use of box–behnen design in an aqueous solution. *Desalination and Water Treatment* 119, 53–63.
- Shokoohi, R., Bajalan, S., Salari, M., Shabanloo, A., 2019. Thermochemical degradation of furfural by sulfate radicals in aqueous solution: optimization and synergistic effect studies. *Environmental Science and Pollution Research* 26 (9), 8914–8927.
- Singh, S., Srivastava, V.C., Mall, I.D., 2009. Fixed-bed study for adsorptive removal of furfural by activated carbon. *Colloids Surf., A* 332 (1), 50–56.
- Souri, Z., Ansari, A., Nematollahi, D., Mazloum-Ardakani, M., 2020. Electrocatalytic degradation of dibenzoazepine drugs by fluorine doped β -PbO₂ electrode: New insight into the electrochemical oxidation and mineralization mechanisms. *J. Electroanal. Chem.* 114037.
- Sözen, S., Olmez-Hanci, T., Hooshmand, M., Orhon, D., 2020. Fenton oxidation for effective removal of color and organic matter from denim cotton wastewater without biological treatment. *Environ. Chem. Lett.* 18 (1), 207–213.
- Takmil, F., Esmacili, H., Mousavi, S.M., Hashemi, S.A., 2020. Nanomagnetically modified activated carbon prepared by oak shell for treatment of wastewater containing fluoride ion. *Adv. Powder Technol.* 31 (8), 3236–3245.
- Wang, C.-T., Hu, J.-L., Chou, W.-L., Kuo, Y.-M., 2008. Removal of color from real dyeing wastewater by Electro-Fenton technology using a three-dimensional graphite cathode. *J. Hazard. Mater.* 152 (2), 601–606.
- Xu, W., Zhao, Q., Wang, R., Jiang, Z., Zhang, Z., Gao, X., et al, 2017. Optimization of organic pollutants removal from soil eluent by activated carbon derived from peanut shells using response surface methodology. *Vacuum* 141, 307–315.
- Yahiaoui, I., Aissani-Benissad, F., Ait-Amar, H., 2010. Optimization of silver cementation yield in fixed bed reactor using factorial design and central composite design. *The Canadian Journal of Chemical Engineering.* 88 (6), 1099–1106.
- Yahiaoui, I., Belattaf, A., Aissani-Benissad, F., Cherif, L.Y., 2011. Full factorial design applied to the biosorption of lead (II) ions from aqueous solution using Brewer's Yeast (*Saccharomyces cerevisiae*). *J. Chem. Eng. Data* 56 (11), 3999–4005.
- Yang, Z.-F., Li, L.-Y., Hsieh, C.-T., Juang, R.-S., 2018. Co-precipitation of magnetic Fe₃O₄ nanoparticles onto carbon nanotubes for removal of copper ions from aqueous solution. *J. Taiwan Inst. Chem. Eng.* 82, 56–63.
- Yang, T., Li, W., Ogunbiyi, A.T., 2021. The effect of Br- and alkali in enhancing the oxidation of furfural to maleic acid with hydrogen peroxide. *Molecular Catalysis.* 504, 111488.
- Yao, Y., Li, M., Yang, Y., Cui, L., Guo, L., 2019. Electrochemical degradation of insecticide hexazinone with Bi-doped PbO₂ electrode: influencing factors, intermediates and degradation mechanism. *Chemosphere* 216, 812–822.
- Zaroual, Z., Azzi, M., Saib, N., Chaïnet, E., 2006. Contribution to the study of electrocoagulation mechanism in basic textile effluent. *J. Hazard. Mater.* 131 (1–3), 73–78.
- Zhang, N., Bu, J., Meng, Y., Wan, J., Yuan, L., Peng, X., 2020. Degradation of p-aminophenol wastewater using Ti-Si-Sn-Sb/GAC particle electrodes in a three-dimensional electrochemical oxidation reactor. *Appl. Organomet. Chem.* 34, (6) e5612.
- Zhang, B., Hou, Y., Yu, Z., Liu, Y., Huang, J., Qian, L., et al, 2019. Three-dimensional electro-Fenton degradation of Rhodamine B with efficient Fe-Cu/kaolin particle electrodes: electrodes optimization, kinetics, influencing factors and mechanism. *Sep. Purif. Technol.* 210, 60–68.
- Zhang, C., Jiang, Y., Li, Y., Hu, Z., Zhou, L., Zhou, M., 2013. Three-dimensional electrochemical process for wastewater treatment: a general review. *Chem. Eng. J.* 228, 455–467.
- Zhao, H.-Z., Sun, Y., Xu, L.-N., Ni, J.-R., 2010. Removal of Acid Orange 7 in simulated wastewater using a three-dimensional electrode reactor: removal mechanisms and dye degradation pathway. *Chemosphere* 78 (1), 46–51.